The Effect of Bottom Pressure Decoupling on the Speed of Extratropical, Baroclinic Rossby Waves

RÉMI TAILLEUX* AND JAMES C. MCWILLIAMS

Institute of Geophysics and Planetary Physics, University of California, Los Angeles, Los Angeles, California

(Manuscript received 23 August 1999, in final form 24 August 2000)

ABSTRACT

In layered models of the ocean, the assumption of a deep resting layer is often made, motivated by the surface intensification of many phenomena. The propagation speed of first-mode, baroclinic Rossby waves in such models is always faster than in models with all the layers active. The assumption of a deep-resting layer is not crucial for the phase-speed enhancement since the same result holds if the bottom pressure fluctuations are uncorrelated from the overlying wave dynamics.

In this paper the authors explore the relevance of this behavior to recent observational estimates of ''too-fast'' waves by Chelton and Schlax. The available evidence supporting this scenario is reviewed and a method that extends the idea to a continuously stratified fluid is developed. It is established that the resulting amplification factor is at leading order captured by the formula,

$$C_{\mathrm{fast}}/C_{\mathrm{standard}} = 1 + \frac{\Phi_1'^2(-H_0)}{\dfrac{1}{H_0}\displaystyle\int_{-H_0}^{0} \Phi_1'^2(z)\, dz} > 1,$$

where C_{fast} is the enhanced phase speed, C_{standard} the standard phase speed, $\Phi_1'(z)$ is the standard first mode for the velocity and pressure, and H_0 is the reference depth serving to define it. In the case WKB theory is applicable in the vertical direction, the above formula reduces to

$$C_{\mathrm{fast}}/C_{\mathrm{standard}} = 1 + \frac{2N_b}{\overline{N}},$$

where N_b is the deep Brunt–Väisälä frequency and $\overline{N}$ its vertical average.

The amplification factor is computed from a global hydrographic climatology. The comparison with observational estimates shows a reasonable degree of consistency, although with appreciable scatter. The theory appears to do as well as the previously published mean-flow theories of Killworth et al. and others. The link between the faster mode and the surface-intensified modes occurring over steep topography previously discussed in the literature is also established.

1. Introduction

a. Motivation and background

In layered models of the ocean the assumption of a deep resting layer is often made, motivated by the surface intensification of many phenomena. The propagation speed of first-mode, baroclinic Rossby waves in such models is always faster than in models with all the layers active. For example, in the so-called reduced-gravity or 1.5-layer model, baroclinic Rossby waves are faster than in the full two-layer model by the factor H/H_2, where H_2 is the lower layer thickness and H the total ocean depth.

This behavior is qualitatively similar to the recent finding by Chelton and Schlax (1996) from TOPEX/Poseidon altimetry that observed extratropical, baroclinic Rossby waves are systematically faster than predicted by the standard linear theory. The discrepancy is illustrated in Fig. 1 (bottom), which displays the ratio of observed to theoretical phase speeds. This ratio is seen to increase poleward and can reach values as high as two to three at high latitudes. Given that the mixed layer and the pycnocline also increase with latitude on average, such a behavior is also expected for H/H_2.

The ''Radon Transform'' method used by Chelton and Schlax (1996) does not distinguish between low- and high-frequency motions within the altimetric dataset that resolves periods of months and longer; this method simply provides a global phase-speed estimate based on

* Current affiliation: LMD—UPMC, Paris, France.

Corresponding author address: Dr. Rémi Tailleux, LMD—UPMC, Paris 6, Case Courrier 99, 4, Place Jussieu, 75252 Paris Cédex 05, France.
E-mail: tailleux@lmd.jussieu.fr

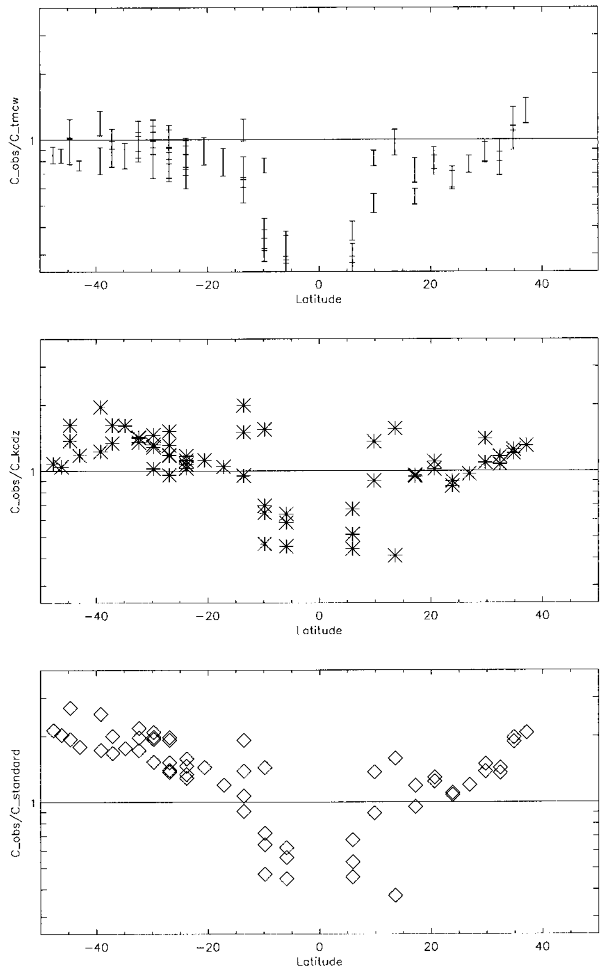

FIG. 1. The ratio of observed to theoretical phase speed for three different theories: (top) pressure-decorrelation theory, (middle) mean-flow theory, (bottom) standard theory. Note the logarithmic scale for the ordinate.

the assumption that the propagation is quasi-nondispersive. Subsequently, Zang and Wunsch (1999) computed frequency/wavenumber diagrams from TOPEX/Poseidon to determine an empirical dispersion relationship for the observed first-mode baroclinic Rossby waves. They found a discrepancy with the standard theory only for the higher frequency motions. This is in agreement with the study by Hong et al. (1998); they did not find enhanced phase speeds necessary to account for decadal sea-level variability in the North Atlantic subtropical gyre. Currently it is unclear what distinguishes these methods of analysis or lower and higher frequency Rossby waves, although the latter seem to have shorter zonal length scales in extratropical regions. In the present study, we focus on motions of subbasin length scale, though still in the nondispersive limit of Rossby wave propagation, hence we only attempt to compare our results with that of Chelton and Schlax (1996). Future studies should include dispersive and finite-domain effects as well to allow a more complete comparison with the frequency/wavenumber analysis of the altimetric data.

There have been several theoretical attempts to explain Chelton and Schlax's (1996) results. The most popular explanation to date is that mean-flow effects account for most of the discrepancy (e.g., Killworth et al. 1997; Dewar 1998; de Szoeke and Chelton 1999; Liu 1999). Estimates from this theory are shown in Fig. 1 (middle panel). They do better than the standard theory but are still systematically too low, suggesting that other effects might also be important.

Among the other theoretical possibilities, the speed doubling mechanism due to a periodic forcing proposed by White (1977) and Qiu et al. (1997) can be rejected because it is only a visual effect that is filtered out by the radon transform method used by Chelton and Schlax (1996). The radon transform is able to distinguish between individual propagating components so that it does not see the sum

$$\cos\omega t + \cos(\omega t + kx)$$

as a spatially modulated wave,

$$2 \cos kx \cos(\omega t + kx/2),$$

propagating at twice the standard-theory speed (as argued by White 1977), but as two waves yielding two peaks. The first has an infinite phase speed, and the second has the standard speed. This is easily verified by running the radon transform on the above expression.

An explanation involving the coupling with the atmosphere is investigated by White et al. (1997), but the analysis is not very convincing due to the coarse-resolution data and the limited time series used. The effect of a smooth topography in a continuously stratified fluid is investigated by Killworth and Blundell (1999) by means of a WKB theory, but the authors do not find a systematic phase-speed enhancement in this case. On the other hand, Tailleux and McWilliams (2000) find a systematic phase-speed enhancement over a steep topography in a two-layer model, a possibility previously raised by Rhines (1977) and Veronis (1981) and related to the faster phase speed of the reduced-gravity model.

The simplest way to address the possibility of phase-speed enhancement in a two-layer model is by examining the evolution equation for the baroclinic mode written as follows:

$$\frac{\partial \eta_2}{\partial t} - \frac{g'\beta H_1}{f^2}\frac{\partial \eta_2}{\partial x} = -\frac{\beta H_1}{f^2}\frac{\partial p_2}{\partial x}, \qquad (1)$$

where p_2 is the bottom pressure, η_2 the displacement of the layers interface, g' the reduced gravity of the density difference across the interface between the layers, H_1 the upper layer thickness, f the Coriolis parameter, and $\beta = df/dy$ its latitudinal derivative; see Tailleux and McWilliams (2000) for details about the derivation of (1). In the standard theory, the bottom pressure is proportional to the interface according to $p_2 = -H_1/H_2\eta_2$ so that the right-hand side contributes to the propagation to define an effective phase speed, $c = -g'\beta H_1 H_2/(f^2 H)$. However, if we assume that for some reason $\partial_x p_2$ is uncorrelated to $\partial_x \eta_2$, then the effective speed becomes $c = -g'\beta H_1/f^2$, which is faster by the factor H/H_2. This condition is obviously realized in a reduced-gravity model that assumes $p_2 = 0$.

In order to assess the relevance of this idea for the interpretation of Chelton and Schlax's (1996) results, we confront two main difficulties. First, we have to decide whether there is a reasonable basis for assuming either bottom pressure compensation or decoupling (i.e., decorrelation from pressure fluctuations in the upper ocean). Second, we need to determine how to estimate the analog of the enhancement factor H/H_2 for a realistic stratified ocean.

b. Basis for bottom pressure decoupling

In Tailleux and McWilliams (2000), the phase-speed enhancement occurs as the result of the decoupling of $\partial_x p_2$ with $\partial_x \eta_2$. In this case, the responsible mechanism is the steep topography. Past studies investigating the effects of the topography on the baroclinic modes have shown the existence of top-trapped modes, but they generally failed to associate this feature with faster propagation (Rhines 1970; Straub 1994; Samelson 1992; Reznik and Tsybaneva 1994; Hallberg 1997).[1]

The possibility of top-trapping does not appear to be uniquely related to the existence of topography. For instance, surface intensification occurs in the calculations of McWilliams et al. (1986) for the nonlinear propagation of a vortex over a flat bottom, with the resulting phase-speed enhancement noted by the authors. However, the physical mechanisms responsible for the surface intensification in these calculations are still largely unexplained. Certainly, the effects of nonlinearities, eddies, small-scale topography, and weak stratification of the deep ocean may all play a role in decoupling the abyss from the upper ocean. Potentially relevant are the concepts of arrested Ekman layers [e.g., see Garrett et al. (1993), Mellor and Wang (1996) and references therein], which can give rise to bottom pressure decoupling when isopycnals intersect topography. We also note that circumstances in which eddy–topography interactions are detuned in the deep ocean have been found in the numerical experiments of two-layer quasigeostrophic (QG) turbulence by Rhines (1975) and Rhines (1977).

The studies cited above compose the present theoretical evidence that bottom pressure compensation or decoupling and/or strong surface intensification frequently occur in the ocean, along with the accompanying phase-speed enhancement. In this paper, we propose a method to estimate the latter effect in a continuously stratified fluid. The pressure-decorrelation estimates are displayed in Fig. 1 (top), along with those from the mean-flow (middle) and standard (bottom) theories, and the pressure-decorrelation estimates are in reasonable agreement with the observational estimates.

[1] However, Samelson (1992) points out that surface-trapped waves have higher frequencies by the ratio H/H_2, whose consequence is higher phase speeds.

c. Quantification of the phase-speed enhancement factor

If one tries to estimate the value of the enhancement factor by using typical values for H and H_2 based on the depth of the pycnocline (e.g., $H_2 = 4000$ m, $H = 5000$ m), H/H_2 appears to be quite small (1.25 in this example) compared to the observed phase-speed enhancement factor of 2 or more (Fig. 1, bottom). According to Flierl (1978), however, the value of H/H_2 depends on which physical process one is interested in modeling accurately. For instance, Flierl (1978) finds that $H_2 = H/2$ is required to model strong topographic effects accurately (thus implying $H/H_2 = 2$), whereas the choice of a much thinner upper layer is better suited to modeling the response to wind forcing. In this paper, we propose a method that eliminates the concern for the right two-layer calibration by focusing on a continuously stratified fluid.

d. Methodology and organization

In order to facilitate a comparison between our approach and those mentioned above, it is useful to proceed by analogy with the situation described by the following schematic dynamical problem:

$$\frac{\partial p}{\partial t} + \mathbf{A}\frac{\partial p}{\partial x} = 0, \qquad (2)$$

where p is a state vector of dimension N, and $\mathbf{A}$ an $N \times N$ square matrix. Within this simple framework, the standard theory is analogous to the case where $\mathbf{A}$ is a diagonal matrix with constant coefficients. In this case, the modal amplitudes (the components p_i of p) are independent of each other, each obeying a scalar equation of the type $\partial_t p_i + c_i \partial_x p_i = 0$. In order to include realistic effects, like that of the mean flow (Killworth et al. 1997) or the topography (Killworth and Blundell 1999), the matrix $\mathbf{A}$ must be transformed into one with variable coefficients, including nonzero off-diagonal ones. As a result, the p_i become coupled. Under the assumption that there is a scale separation between the spatial variations of the environment and that of the waves, which justifies the use of WKB theory, this coupling can be interpreted in terms of anomalous propagation. In this case, the coupled modes and their phase speeds are simply determined by diagonalizing the matrix $\mathbf{A}$.

Implicit in the above-mentioned theories is that the matrix $\mathbf{A}$ is somehow perfectly known. As a result, the q_i are expected to be well-behaved deterministic quantities, with well-defined spatial and temporal characteristics. However, this might not be the case. Indeed, one may easily conceive that the neglected nonlinearities, small scales, temporal variations, etc. if included, would have a significant impact on the dynamics of the system. In this paper, we assume that the main consequence of neglecting the above effects is to render aspects of the model dubious and inaccurate. Our strategy thus consists in modifying this dubious dynamics by an additional constraint that we believe may often be more accurate. In some ways this strategy is equivalent to making a closure assumption. In this paper, we assume that a particular combination of the p_i that constitute the bottom pressure has, in fact, the behavior of a random variable. In other words, we add to the usual dynamics a constraint of the form $\Sigma_{j=0}^{N} s_j p_j = X(x, t)$, with X a random process with unspecified characteristics and s_j constants discussed later in the text. This constraint allows the expression of one of the p_i, p_N say, in terms of the others. After substitution of this constraint, our schematic problem (2) is transformed into one of the form,

$$\frac{\partial p^*}{\partial t} + \mathsf{A}^*\frac{\partial p^*}{\partial x} = \mathbf{F}(x, t), \tag{3}$$

where $p^* = (p_1, \cdots, p_{N-1})$ has one component less than p; A^* is a $(N - 1)$-dimensional square matrix; and $\mathbf{F}(x, t)$ is a random vector. In this paper, we argue that the new wave properties are to be obtained by diagonalizing A^*, not A.

This paper is organized as follows: The coupled equations for the planetary geostrophic standard modes over topography that result from making the bottom pressure decoupling hypothesis are presented in section 2. The theory for the phase-speed enhancement resulting from bottom pressure decoupling and application to several illustrative examples are presented in section 3. The issue of the vertical structure of the modes is addressed in section 4. A comparison of our predictions with the observational estimates is presented in section 5. A discussion concludes the paper in section 6.

2. Planetary geostrophic equations

As stated in the introduction, we are interested in investigating how the coupling of the standard modes resulting from any departure from the idealized assumptions of the standard linear model—flat bottom, horizontally uniform stratification, free, inviscid, small perturbations to a state of rest, etc.—may modify the propagation properties of the planetary Rossby modes. Of course, all the effects neglected in the standard theory—forcing, dissipation, topography, nonlinearities, etc.—contribute to the coupling, so that the most general problem is quite complicated. For the reasons given in the introduction, we shall focus here on the topography effects only.

a. Dynamical model

Our starting point is the standard linear model, composed by the linearized primitive equations in absence of forcing and dissipation,

$$\frac{\partial \mathbf{u}}{\partial t} + f\hat{\mathbf{z}} \times \mathbf{u} + \boldsymbol{\nabla} p = 0 \tag{4}$$

$$\frac{\partial p}{\partial z} = b \tag{5}$$

$$\frac{\partial u}{\partial x} + \frac{\partial v}{\partial y} + \frac{\partial w}{\partial z} = 0 \tag{6}$$

$$\frac{\partial b}{\partial t} + N^2 w = 0. \tag{7}$$

The notation is standard: $\mathbf{u} = (u, v)$ denotes the horizontal velocity; w the vertical velocity; $p = P/\rho_0$ the pressure divided by a reference density ρ_0; $b = -g\rho/\rho_0$ the buoyancy, with g the gravitational acceleration and ρ the density; $N^2(z) = -(g/\rho_0)d\overline{\rho}_0/dz$ the Brunt–Vaisälä frequency computed from the mean density profile $\overline{\rho}_0(z)$; f the Coriolis parameter; and $\beta = df/dy$ the latitudinal derivative of f. These equations are supplemented by the linearized boundary conditions,

$$\left.\begin{aligned} w &= \frac{\partial \eta}{\partial t} \\ p &= g\eta \end{aligned}\right\} \qquad \text{at } z = 0, \tag{8}$$

$$w = -\mathbf{u} \cdot \boldsymbol{\nabla} H \quad \text{at } z = -H(x, y), \tag{9}$$

where $\eta(x, y, t)$ denotes the departure of the sea surface height from its resting position $z = 0$, while $z = -H(x, y)$ denotes the position of the ocean bottom. From a mathematical viewpoint, the only departure from the standard linear theory lies in the bottom boundary condition (9) used in place of the standard (i.e., flat-bottom boundary condition) $w(-H_0) = 0$.

b. Projection onto the standard modes

For any given reference standard depth H_0 [taken here as the maximum value of $H(x, y)$] and background stratification with buoyancy frequency $N(z)$, the standard normal modes are defined as the eigenmodes of the following Sturm-Liouville problem:

$$\frac{d^2\Phi_k}{dz^2} + \frac{N^2}{c_k^2}\Phi_k = 0, \tag{10}$$

with boundary conditions,

$$\Phi_k'(0) = \frac{g}{c_k^2}\Phi_k(0), \qquad \Phi_k(-H_0) = 0 \tag{11}$$

(Gill 1982). As is well known, the square root of the constant of separation c_k can be interpreted as the phase speed of the gravity wave modes of the system. The set of modes $\Phi_k'(z)$, obtained by taking the vertical derivative of $\Phi_k(z)$, form a complete orthogonal basis that can be used to express the horizontal velocity and pressure fields as the following series expansions:

$$\mathbf{u}(x, y, z, t) = \sum_{k=0}^{+\infty} \mathbf{U}_k(x, y, t)\Phi_k'(z) \tag{12}$$

$$p(x, y, z, t) = \sum_{k=0}^{+\infty} \Pi_k(x, y, t)\Phi_k'(z). \tag{13}$$

The hydrostatic approximation (5) allows us to obtain the buoyancy from p by taking the vertical derivative of (13). Simplifying the result by means of (10) yields

$$b(x, y, z, t) = -N^2(z) \sum_{k=0}^{+\infty} c_k^{-2}\Pi_k(x, y, t)\Phi_k(z). \tag{14}$$

Integrating the continuity equation (6) over depth and accounting for the bottom boundary condition (9) allows us to diagnose the vertical velocity from the horizontal velocity as follows:

$$w(x, y, z, t) = -\mathrm{div} \int_{-H}^{z} \mathbf{u}(x, y, \zeta, t)\, d\zeta. \tag{15}$$

Inserting (12) into (15) yields the following series expansion for w:

$$w(x, y, z, t) = \mathcal{C}(x, y, t) - \sum_{k=0}^{+\infty} \mathrm{div}\mathbf{U}_k(x, y, t)\Phi_k(z), \tag{16}$$

where the function $\mathcal{C}(x, y, t)$ is defined by

$$\mathcal{C}(x, y, t) = \mathrm{div}\left[\sum_{k=0}^{+\infty} \Phi_k(-H)\mathbf{U}_k\right]. \tag{17}$$

The term $\mathcal{C}$ involves the values of Φ_k at $z = -H(x, y)$, so it would vanish in the standard theory. It is therefore responsible for the modal coupling here. We can get a sense of the physical meaning of $\mathcal{C}$ by expanding $\Phi_j(-H)$ in a Taylor series,

$$\Phi_j(-H_0) = \Phi_j(-H) - (H_0 - H)\Phi_j'(-H) + \cdots, \tag{18}$$

which vanishes from (11). It follows that at leading order $\Phi_j(-H) \approx (H_0 - H)\Phi_j'(-H)$ so that $\mathcal{C}$ becomes

$$\mathcal{C}(x, y) \approx \mathrm{div}\left(\sum_{k=0}^{+\infty} \Phi_k'(-H)\mathcal{B}\mathbf{U}_k\right) = \mathrm{div}(\mathcal{B}\mathbf{U}_b), \tag{19}$$

where $\mathcal{B} = H_0 - H(x, y)$ is the topographic anomaly and $\mathbf{U}_b$ the bottom velocity. In cases where the bottom velocity is in approximate geostrophic balance, $\mathcal{C}$ reduces to

$$\mathcal{C}(x, y) = J\left(\frac{\mathcal{B}}{f}, p_b\right) \tag{20}$$

with p_b the bottom pressure. Equation (20) shows that $\mathcal{C}$ is closely related to the bottom pressure torque appearing in joint effect of baroclinicity and relief (JEBAR) theories. This is expected, because JEBAR appears in any formulation that decomposes the circulation into a vertically averaged part (the standard barotropic mode) plus a part with zero vertical average (the sum of all the baroclinic modes), which is equivalent to the present approach. In the following, no use will be made of (20) because our derivations are independent of the precise form of $\mathcal{C}$, as we show below.

In order to obtain the coupled modal equations, we first insert the expressions (16) and (14) into the buoyancy equation (7), yielding

$$\sum_{k=0}^{+\infty} \left(\frac{1}{c_k^2}\frac{\partial \Pi_k}{\partial t} + \mathrm{div}\mathbf{U}_k\right)N^2(z)\Phi_k(z) = N^2(z)\mathcal{C}(x, y, t). \tag{21}$$

The surface boundary condition (8) imposes $w(0) = g^{-1}\partial p/\partial t(0)$. Using (13) and (16), this yields

$$\sum_{k=0}^{+\infty} \Phi_k'(0)\frac{\partial \Pi_k}{\partial t} = -g\left(\sum_{k=0}^{+\infty} \mathrm{div}\mathbf{U}_k\Phi_k(0) - \mathcal{C}\right). \tag{22}$$

From (11), this can be rewritten as follows:

$$\sum_{k=0}^{+\infty} \left(\frac{1}{c_k^2}\frac{\partial \Pi_k}{\partial t} + \mathrm{div}\mathbf{U}_k\right)\Phi_k(0) = \mathcal{C}(x, y, t). \tag{23}$$

A second set of equations is obtained by inserting (12) and (13) into the horizontal momentum equations (4); namely,

$$\sum_{k=1}^{+\infty} \left(\frac{\partial \mathbf{U}_k}{\partial t} + f\hat{\mathbf{z}} \times \mathbf{U}_k + \nabla\Pi_k\right)\Phi_k'(z) = 0. \tag{24}$$

Equations (21), (23), and (24) are projected onto the normal modes by using the following orthogonality conditions:

$$\int_{-H_0}^{0} N^2\Phi_i(z)\Phi_j(z)\, dz + g\Phi_i(0)\Phi_j(0) = \int_{-H_0}^{0} \Phi_j'(z)\Phi_i'(z)\, dz = 0 \tag{25}$$

when $i \neq j$. As a result, the sought-for coupled modal equations are given by

$$\frac{\partial \mathbf{U}_j}{\partial t} + f\hat{\mathbf{z}} \times \mathbf{U}_j + \nabla\Pi_j = 0 \tag{26}$$

$$\frac{\partial \Pi_j}{\partial t} + c_j^2\, \mathrm{div}\mathbf{U}_j = \Gamma_j\mathcal{C}(x, y, t) \tag{27}$$

with

$$\Gamma_j = c_j^2\frac{\int_{-H_0}^{0} N^2(z)\Phi_j(z)\, dz + g\Phi_j(0)}{\int_{-H_0}^{0} N^2(z)\Phi_j^2(z)\, dz + g\Phi_j^2(0)}. \tag{28}$$

As in Tailleux and McWilliams (2000), we focus on planetary geostrophic motions with slow timescales (on the order of a month and longer) and spatial scales large compared to the first baroclinic Rossby radius of deformation. As a result, one can replace (26) by the geostrophic approximation. Furthermore, in the case of the barotropic case ($j = 0$), one can also neglect the time derivative in (27), which yields the classical Sverdrup balance. These classical approximations permit the simplification of (26) and (27) as follows:

$$-\frac{\beta g H_0}{f^2}\frac{\partial \Pi_0}{\partial x} = \Gamma_0 \mathcal{C}(x, y), \tag{29}$$

$$\frac{\partial \Pi_j}{\partial t} - \frac{\beta c_j^2}{f^2}\frac{\partial \Pi_j}{\partial x} = \Gamma_j \mathcal{C}(x, y), \qquad j \geq 1, \tag{30}$$

where (29) is the Sverdrup balance for the barotropic mode and (30) the coupled equations for the baroclinic modes. This set of equations generalizes to an infinite number of modes the two-layer equations used in Tailleux and McWilliams (2000) and constitute the starting point of the following analysis. In this case, the barotropic vorticity balance is between the meridional advection of planetary vorticity and the JEBAR term. In absence of the latter, the baroclinic equations (30) would simply correspond to nondispersive wave propagation with the standard westward phase speed $\beta c_j^2/f^2 = \beta R_j^2$, with R_j the jth baroclinic Rossby radius of deformation.

c. The hypothesis of bottom pressure decorrelation

We proceed by analogy with the two-layer example discussed in the introduction. The main objective is to obtain a suitable form of the system (29)–(30) allowing us to introduce naturally the bottom pressure decorrelation hypothesis discussed above. To that end, the main idea is to confine any explicit reference to the bottom topography to only one equation. Indeed, if one inspects the system (29)–(30), one realizes that all the equations depend explicitly on the topography through the term $\mathcal{C}$, as the form (20) establishes clearly. This is quite unsatisfactory given the present state of uncertainty regarding what essential characteristics of H should be retained for modeling purposes. For this reason, we first use (29) to express $\mathcal{C}$ in terms of the barotropic mode and insert the result into all the baroclinic equations (30). This yields the system

$$-\frac{\beta g H_0}{f^2}\frac{\partial \Pi_0}{\partial x} = \Gamma_0 \mathcal{C}, \tag{31}$$

$$\frac{\partial \Pi_j}{\partial t} - \frac{\beta c_j^2}{f^2}\frac{\partial \Pi_j}{\partial x} = -\frac{\Gamma_j}{\Gamma_0}\frac{\beta g H_0}{f^2}\frac{\partial \Pi_0}{\partial x}, \tag{32}$$

which is strictly equivalent to (29)–(30), with the important difference that explicit reference to the bottom topography is now solely confined to (31). The main advantage of (32) is that all the coefficients that appear in it depend uniquely on integral properties of the standard modes and thus depend uniquely on the background stratification and reference depth H_0. Since we are much more confident about how to choose $N^2(z)$ and H_0 than $H(x, y)$ in the actual ocean, we believe that the equations constituting (32) have more informative content and a more deterministic character than (30) and (31).

In order to introduce the bottom pressure decorrelation hypothesis, we need to insert information about the bottom pressure into the system (32). To that end, we first express the bottom pressure p_b in terms of the normal modes. From (13), one has

$$\begin{aligned} p_b(x, y, t) &= p(x, y, z = -H, t) \\ &= \sum_{k=0}^{+\infty} \Pi_k(x, y, t)\Phi_k'(-H). \end{aligned} \tag{33}$$

From a Taylor series expansion, we can see that $\Phi_k'(-H) = \Phi_k'(-H_0) + O(\mathcal{B}^2)$ [because $\Phi_k''(-H_0) = 0$ from (10) and (11)] so that $\Phi_k'(-H)$ differs from $\Phi_k'(-H_0)$ only at second order in the topography anomaly. For simplicity, we shall make this approximation in the following. Note that the approximation $\Phi_k'(-H) = \Phi_k'(-H_0)$ is exact for the barotropic mode ($k = 0$) since $\Phi_0(z)$ varies linearly with depth. Equation (33) allows the barotropic amplitude Π_0 to be expressed in terms of p_b and the baroclinic amplitude Π_j, $j \geq 1$. Inserting the result into (32) yields

$$\frac{\partial \Pi_j}{\partial t} - \frac{\beta c_j^2}{f^2}\frac{\partial \Pi_j}{\partial x} \approx -\frac{\Gamma_j}{\Gamma_0}\frac{\beta g H_0}{f^2}\frac{\partial}{\partial x}\left[\frac{p_b - \sum_{k=1}^{+\infty}\Phi_k'(-H_0)\Pi_k}{\Phi_0'(-H_0)}\right]. \tag{34}$$

We rewrite this equation under the form

$$\frac{\partial \Pi_j}{\partial t} - \frac{\beta}{f^2}\left[c_j^2\frac{\partial \Pi_j}{\partial x} + \sum_{k=1}^{+\infty}\sigma_{jk}\frac{\partial \Pi_k}{\partial x}\right] = -\frac{\Gamma_j}{\Gamma_0}\frac{\beta g H_0}{f^2\Phi_0'(-H_0)}\frac{\partial p_b}{\partial x}, \tag{35}$$

where

$$\sigma_{jk} = \frac{\Gamma_j\Phi_k'(-H_0)}{\Gamma_0\Phi_0'(-H_0)}gH_0. \tag{36}$$

The system (35) is the generalization to an infinite number of modes of the two-layer model Eq. (1) discussed in the introduction. If needed, the consistency between the two approaches is further demonstrated in section 3b.

As stated in the introduction, this paper argues that the randomness of the topography introduces a randomness in the system whose main consequence is to render (31) greatly uncertain and inaccurate. Since (31) and (35) are coupled, it follows that randomness must also be present in (35). On the physical grounds detailed in the introduction, which mainly stem from our previous analysis of the two-layer model solutions reported in Tailleux and McWilliams (2000), we believe that the main consequence of this randomness is that the right-hand side of (35) does not have any influence on propagating solutions of the system. It follows that the anomalous propagation due to the departure from the idealized assumptions of the standard linear model considered here can be understood by analyzing the propagation properties of (35) with the right-hand side taken as zero.

3. Propagation analysis

a. General theory

The system (35), with $j \geq 1$, is an infinite-dimensional system. We analyze its properties by considering successive truncations. The truncated system of order n, obtained by retaining only the terms $k = 1, \cdots, n$ in the infinite series in (35), is of the following form:

$$\frac{\partial \mathbf{\Pi}}{\partial t} - \frac{\beta}{f^2}\mathsf{M}_n\frac{\partial \mathbf{\Pi}}{\partial x} = -\frac{\beta g H_0}{\Phi_0'(-H_0)}\frac{\partial p_b}{\partial x}\mathbf{\Gamma}, \qquad (37)$$

with the coefficients of the $n \times n$ matrix M_n being $m_{jk} = \sigma_{jk} + c_j^2\delta_{jk}$, $j = 1, \cdots, n$, $k = 1, \cdots, n$; δ_{jk} the Kronecker δ; $\mathbf{\Gamma}$ the n-dimensional vector with components Γ_j/Γ_0, $j = 1, \cdots, n$; and $\mathbf{\Pi}$ the n-dimensional vector of components Π_j, $j = 1, \cdots, n$. As stated previously, we assume that the right-hand side of (37) does not contribute to the propagation of the wave modes. Thus, the propagation properties of (37) are obtained by diagonalizing the matrix M_n, with the enhanced phase speed given by the greatest eigenvalue.

1) THE COEFFICIENTS σ_{jk}

In order to compute the eigenvalues of the matrix M_n, the coefficients σ_{jk} are needed. As seen in the previous section, those are given by the expression (36) whose definition involves the coefficients Γ_j (28). We first simplify the expression for the latter by establishing the two relations

$$\begin{aligned}\int_{-H_0}^{0} N^2\Phi_j(z)\,dz + g\Phi_j(0) &= c_j^2(\Phi_j'(-H_0) - \Phi_j'(0)) \\ &\quad + g\Phi_j(0) \\ &= c_j^2\Phi_j'(-H_0), \end{aligned} \qquad (38)$$

$$\int_{-H_0}^{0} N^2\Phi_j^2(z)\,dz + g\Phi_j^2(0) = c_j^2\int_{-H_0}^{0}\Phi_j'^2(z)\,dz. \qquad (39)$$

The first is obtained by integrating (10) over depth, while the second is obtained by integrating (10) multiplied by Φ_j over depth, in both cases accounting for the boundary conditions (11). By using these two expressions, (28) becomes

$$\Gamma_j = c_j^2\frac{\Phi_j'(-H_0)}{\displaystyle\int_{-H_0}^{0}\Phi_j'^2(z)\,dz}. \qquad (40)$$

The expression (36) also involves quantities related to the barotropic mode $\Phi_0(z)$. We estimate those by making the classical approximation consisting in regarding $\Phi_0'(z)$ as independent of depth so that $\Phi_0'(z) = B_0$ with B_0 a constant. As a result, $\Phi_0'(-H_0) = B_0$ and $\int_{-H_0}^{0}\Phi_0'^2(z)\,dz = H_0B_0^2$. From (40) one thus computes $\Gamma_0 = g/B_0$, yielding

$$\frac{gH_0}{\Gamma_0\Phi_0'(-H_0)} = H_0. \qquad (41)$$

By combining the above results to simplify (36), the latter becomes

$$\sigma_{jk} = H_0\Gamma_j\Phi_k'(-H_0) = H_0\frac{\Phi_j'(-H_0)\Phi_k'(-H_0)}{\displaystyle\int_{-H_0}^{0}\Phi_j'^2(z)\,dz}c_j^2. \qquad (42)$$

2) SYMMETRIZATION OF THE PROBLEM

Given an arbitrarily normalized basis of eigenmodes $\tilde{\Phi}_j$, $j = 0, 1, \cdots,$ the expression for σ_{jk} in a different basis Φ_j such that $\Phi_j = B_j\tilde{\Phi}_j$, with B_j a constant, will be, according to (42),

$$\sigma_{jk} = \frac{H_0B_k}{B_j}\frac{\tilde{\Phi}_j'(-H_0)\tilde{\Phi}_k'(-H_0)}{\displaystyle\int_{-H_0}^{0}\tilde{\Phi}_j'^2(z)\,dz}c_j^2. \qquad (43)$$

It is mathematically straightforward to show that the constants B_j only affect the eigenvectors of M_n, but not its eigenvalues. Since symmetric eigenvalue problems are the easiest to solve numerically, we therefore chose the B_j that render M_n symmetric. Thus, solving $\sigma_{jk} = \sigma_{kj}$ for B_j/B_k yields

$$\sigma_{jk} = \frac{\Phi_j'(-H_0)\Phi_k'(-H_0)}{\sqrt{\dfrac{1}{H_0}\displaystyle\int_{-H_0}^{0}\Phi_j'^2(z)\,dz}\sqrt{\dfrac{1}{H_0}\displaystyle\int_{-H_0}^{0}\Phi_k'^2(z)\,dz}}c_jc_k. \qquad (44)$$

Note that we have inserted the factor H_0 in (43) in the square roots of the denominator.

3) LEADING-ORDER PHASE-SPEED ENHANCEMENT

In practice the eigenvalues of M_n for n large have to be estimated numerically. To shed some light on the problem, however, it is of interest to derive the formal anomalous phase speed at the lowest order of truncation. In this case, M_1 is simply the scalar

$$M_1 = c_1^2 + \sigma_{11}, \qquad (45)$$

corresponding to a phase-speed enhancement $1 + \sigma_{11}/c_1^2$. Computing σ_{11} from (44) yields

$$1 + \frac{\sigma_{11}}{c_1^2} = 1 + \frac{\Phi_1'^2(-H_0)}{\frac{1}{H_0}\int_{-H_0}^{0} \Phi_1'^2(z)\, dz} > 1. \quad (46)$$

This formula shows that the anomalous phase speed at the lowest order of truncation is always greater than the standard phase speed. The enhancement factor is seen to depend primarily on the bottom values of $\Phi_1'(z)$, so it is linked to the bottom value of the velocity and pressure perturbations. In order to better understand the nature of the phase-speed enhancement, we consider next three specific cases corresponding to buoyancy profiles with distinct characteristics. First, the singular case of a two-layer stratification is considered as a consistency check. Second, the case of a slowly-varying N^2, which allows WKB theory to be used to derive approximations to σ_{jk}, is considered. Third, the case of an exponential stratification, for which WKB theory fails, concludes our investigation.

b. Application 1: Two-layer stratification

As an initial consistency check, we apply our theory to the case of the two-layer stratification discussed in the introduction. This case corresponds to the particular case of a buoyancy frequency profile whose mathematical expression is

$$N^2(z) = g'\delta(z + H_1), \quad (47)$$

where g' is the reduced gravitational acceleration, H_1 is the upper-layer thickness, and δ the classical Dirac distribution. This singular profile admits only two eigenmodes. With the usual approximations, the barotropic mode takes the form $\Phi_0(z) = B_0(z + H_0)$, while the baroclinic mode is given by $\Phi_1(z) = B_1(z + H_0)$ $(-H_0 \le z \le -H_1)$, $\Phi_1(z) = -B_1H_2/H_1z$ $(-H_1 \le z \le 0)$. These expressions for Φ_0 and Φ_1 are used to compute the coefficients Γ_0 and Γ_1,

$$\Gamma_0 = c_0^2\frac{\Phi_0'(-H_0)}{\int_{-H_0}^{0} \Phi_0'^2(z)\, dz} = \frac{g}{B_0},$$

$$\Gamma_1 = c_1^2\frac{\Phi_1'(-H_0)}{\int_{-H_0}^{0} \Phi_1'^2(z)\, dz} = \frac{H_1}{B_1H_2H_0}c_1^2,$$

and then σ_{11},

$$\sigma_{11} = \frac{\Gamma_1\Phi_1'(-H_0)}{\Gamma_0\Phi_0'(-H_0)}gH_0 = \frac{H_1}{H_2}c_1^2.$$

Since this problem possesses only two eigenmodes, the leading order problem,

$$c_{1,\text{faster}}^2 = c_1^2 + \sigma_{11} = \left(1 + \frac{H_1}{H_2}\right)c_1^2 = \frac{H_0}{H_2}c_1^2, \quad (48)$$

is therefore exact. This amplification factor is the expected result.

c. Application 2: Slowly varying stratification

When N^2 is a slowly varying function of depth in the usual WKB sense, approximate expressions for the standard normal modes can be obtained by making use of WKB theory. Such a method was recently used with success by Chelton et al. (1998) to study the spatial variations of the first baroclinic modes in the ocean, thus indicating that WKB theory can be used for N^2 profiles typical of the real ocean. When WKB theory is applicable, we show in the appendix that the approximate WKB expression for the σ_{jk} is given by

$$\sigma_{jk} \approx \frac{2N_b}{\overline{N}}\frac{1}{jk}c_1^2 = \frac{2N_b}{\overline{N}}c_jc_k, \quad (49)$$

where N_b denotes the value of the Brunt–Vaisälä frequency near the ocean bottom and $\overline{N}$ the vertical average of the Brunt–Vaisälä frequency. The formal solution (46) for the phase-speed enhancement at the lowest order truncation is readily estimated from (49), yielding

$$1 + \frac{\sigma_{11}}{c_1^2} = 1 + \frac{2N_b}{\overline{N}}. \quad (50)$$

In this approximation, one sees that the phase-speed enhancement depends critically on the value of the deep Brunt–Vaisälä frequency. It follows that (50) can only be valid if N_b remains large enough since cases for which N comes close to zero would correspond to a turning point situation where WKB theory is known to fail. One can intuitively understand that (50) breaks down for N_b too small since from (10) one has $\Phi_m''(z) \approx 0$, where $N \ll 1$, Φ_m must be approximately linear in such regions. In such situation, Φ_m behaves independently of the local values of N, so one does not except $\Phi_1(-H_0)$ to depend on N_b. As a result, (50) must greatly underestimate the phase speed enhancement if $N_b \approx 0$. We shall further clarify this issue in the following section.

The next step is to estimate the effects of retaining more terms in the truncation on the phase-speed enhancement. To that end, we first note that (49) allows $\mathbf{M}_n$ to be written under the particularly simple form

$$\mathbf{M}_n = c_1^2(\mathbf{I}_n + \xi\mathbf{J}_n), \quad (51)$$

with $\mathbf{I}_n$ the $n \times n$ matrix of coefficients $I_{jk} = \delta_{jk}/(jk)$ (δ_{jk} being the Kroenecker delta), $\mathbf{J}_n$ the matrix of coefficients $J_{jk} = 1/(jk)$, and $\xi = 2N_b/\overline{N}$. Equation (51) shows that the phase-speed enhancement can be obtained by computing the largest eigenvalue of the matrix $\mathbf{I}_n + \xi\mathbf{J}_n$. It also shows that the amplification factor depends uniquely on the physical parameter ξ for all n. We computed the largest eigenvalue of $\mathbf{I}_n + \xi\mathbf{J}_n$ for n varying between

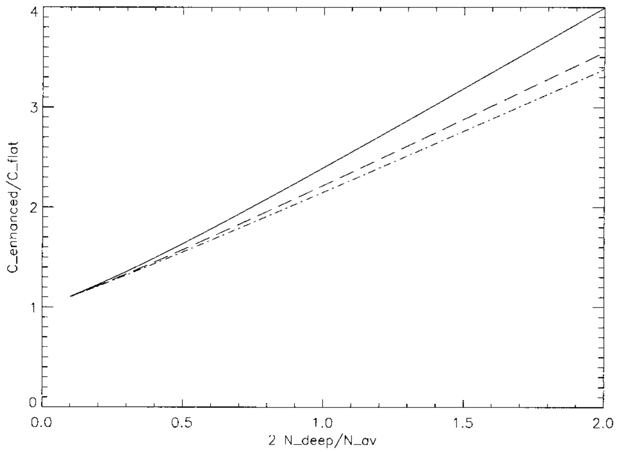

FIG. 2. The amplification factor as a function of $2N_b/\overline{N}$ for different orders of truncation: two modes (dotted–dashed line), three modes (dashed line), and 300 modes (solid line). The amplification factor for even higher orders of truncation is indistinguishable from the solid line, indicating that convergence has been achieved.

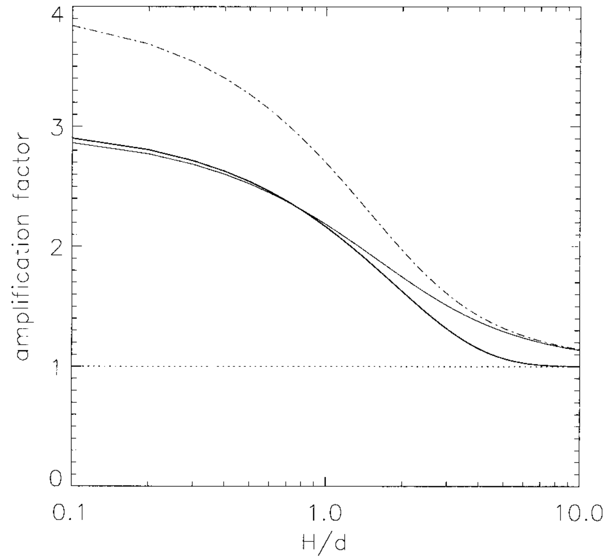

FIG. 3. Theoretical amplification factors for the exponential stratification profile as a function of the ratio H_0/δ: prediction of zero-order WKB theory (thick solid line) computed from Eq. (50), prediction of formal zero order theory (thin solid line) computed from Eq. (46), and prediction obtained by solving the modified Sturm-Liouville problem as explained at the end of section 4 (dotted–dashed line).

2 and 300 by standard numerical methods, for ξ regularly sampled between 0 and 2. In Fig. 2 we display the amplification factor as a function of ξ for the three cases $n = 2$, $n = 3$, and $n = 300$. For greater values of n, the resulting curves are indistinguishable from that corresponding to $n = 300$, indicating that convergence has been achieved. We note that all the curves differ little from each other for $\xi \leq 1$, which corresponds to a ratio $N_b/\overline{N} \leq 0.5$. The maximum error between the linear relation $1 + \xi$ and the asymptotic amplification factor occurs for $\xi = 2$, where the latter reaches the value of 4, while the former is only 3. The value $\xi = 2$ corresponds to the case $N_b = \overline{N}$, that is, the case $N^2 = \text{const}$.

d. Application 3: Exponential stratification

In order to better appreciate when the WKB approximation (50) breaks down as a result of N_b becoming too small, we analyze the idealized case of an exponential stratification,

$$N(z) = N_0 e^{z/\delta}, \tag{52}$$

where N_0 is the surface value and δ the e-folding scale. For large values of H_0/δ, one verifies that (52) will in general violate the conditions (72) in the deep ocean. On the other hand, we expect the WKB expression (50) to remain valid for low values of H_0/δ. In this paragraph, we seek to understand how (50) compares with the more accurate (46). For N given by (52), (50) becomes

$$\left(1 + \frac{\sigma_{11}}{c_1^2}\right)_{\text{WKB}} = 1 + \xi = 1 + \frac{2H_0}{\delta}\frac{e^{-H_0/\delta}}{1 - e^{-H_0/\delta}} \tag{53}$$

and is seen to depend uniquely on the ratio H_0/δ. We compare (53) with the more general (46),

$$\left(1 + \frac{\sigma_{11}}{c_1^2}\right)_{\text{exact}} = 1 + \frac{\Phi_1'^2(-H_0)}{\dfrac{1}{H_0}\displaystyle\int_{-H_0}^{0} \Phi_1'^2(z)\, dz} \tag{54}$$

with $\Phi_1'(z)$ being estimated numerically by solving the Sturm-Liouville problem (10) with N given by (52). The two formula were computed for H_0/δ varying between 0.1 and 10. The result, depicted in Fig. 3, shows the expected difference for high values of H_0/δ the two approaches becoming similar for $H_0/\delta \approx 1$. For comparison, we also added the curve corresponding to the ‘‘exact’’ amplification factor for this particular stratification, which would be obtained in the asymptotic limit of an infinite number of modes. A simple method to compute this limit is given at the end of the following section.

4. Interpretation of the nonstandard modes

A legitimate question is what is the vertical structure of the faster modes. The main result of this section is to link the present modes to the eigenmodes of the standard Sturm-Liouville problem for which the bottom boundary condition of vanishing vertical velocity is replaced by that of vanishing pressure. These modes correspond to the surface-intensified Rossby waves occurring over steep topography, which have been extensively discussed by Rhines (1970), Veronis (1981), Charney and Flierl (1981), and Straub (1994) among others. The following paragraphs present a demonstration of this result in three steps. First, we formally derive the theoretical series expansion for the vertical structure of the faster modes. Second, this series expansion is computed numerically for the case N^2 = const and compared with the solution of the Sturm-Liouville problem with vanishing bottom pressure. Third, the result is demonstrated in the general case.

a. Formal general solution

In order to determine the vertical structure of the nonstandard modes, we first need to understand more about the general solution for the pressure perturbation p. To that end, we first rewrite Eq. (37) more concisely as follows:

$$\frac{\partial \mathbf{\Pi}}{\partial t} - \frac{\beta}{f^2} M_n \frac{\partial \mathbf{\Pi}}{\partial x} = \mathcal{F}, \tag{55}$$

with $\mathcal{F}$ to be regarded as a forcing term. From the theory of forced linear systems, the general solution of (37) is the sum of a particular solution satisfying (55) plus an arbitrary linear combination of solutions of the associated homogeneous problem. Without loss of generality, the solutions of the homogeneous system are taken as plane waves with period ω. Thus, if R_i and μ_i denote the ith eigenvector and eigenvalue of M_n, the general solution of (55) takes the form

$$\mathbf{\Pi} = \mathbf{\Pi}_{\rm part} + \sum_{l=1}^{n} s_l R_l e^{i(k_l x + \omega t)}, \tag{56}$$

where s_l is a constant, $k_l = \omega f^2/(\beta \mu_l)$, and $\mathbf{\Pi}_{\rm part}$ a particular solution satisfying the equation

$$\frac{\partial \mathbf{\Pi}_{\rm part}}{\partial t} - \frac{\beta}{f^2} M_n \frac{\partial \mathbf{\Pi}_{\rm part}}{\partial x} = \mathcal{F}. \tag{57}$$

Inserting (56) into (13) allows the general solution to be written for the pressure perturbation p as the following series expansion:

$$p(x, y, z, t) = p_{\rm part} + \Pi_0(x, y, t)\Phi_0'(z) + \sum_{j=1}^{n}\left(\sum_{l=1}^{n} s_l R_{j,l} \Phi_j'(z) e^{i(k_l x + \omega t)}\right), \tag{58}$$

where $R_{j,l}$ is the jth component of the eigenvector $\mathbf{R}_l$. After permuting the two sums, the above expression becomes

$$\begin{aligned} p(x, y, z, t) &= p_{\rm part} + \Pi_0(x,y,t)\Phi_0'(z) + \sum_{l=1}^{n} s_l e^{i(k_l x+\omega t)}\left(\sum_{j=1}^{n} R_{j,l}\Phi_j'(z)\right) \\ &= p_{\rm part} + \Pi_0(x,y,t)\Phi_0'(z) + \sum_{l=1}^{n} s_l e^{i(k_l x+\omega t)}\Phi_{l,\rm new}'(z), \end{aligned} \tag{59}$$

where the notation

$$\Phi_{l,\rm new}'(z) = \sum_{j=1}^{n} R_{j,l}\Phi_j'(z) \tag{60}$$

has been introduced. Although it would only seem natural to identify the new mode $\Phi_{l,\rm new}$ as the vertical structure associated to the lth anomalous mode (the case l = 1 therefore corresponds to the structure of the "faster" first baroclinic mode), one needs to be aware that the term proportional to Π_0 might also contribute to it. Indeed, any term contained in Π_0 proportional to $e^{i(k_l x+\omega t)}$ would combine to $\Phi_{l,\rm new}$ to give a different vertical structure. We note, however, that $\Phi_0'(z)$ is independent of depth (since it represents the vertical structure of the standard barotropic mode) so that the effect is only to shift the mean value of $\Phi_{l,\rm new}'(z)$. Obviously, the ambiguity arises because our approach replaces one deterministic equation of the initial system by a statement of randomness for the bottom pressure, with a resulting loss of information. It follows that removing the ambiguity would require making further assumptions beyond the scope of this paper. For this reason, we shall restrict ourselves to understanding the nature of $\Phi_{l,\rm new}'(z)$, keeping in mind that the true (if any) vertical structure should be shifted by an unknown constant.

b. Application to the case N^2 = const

In order to illustrate the above concepts, we compute the vertical structure $\Phi_{l,\rm new}'(z)$ for $l = 1$, in the case of a constant N^2. After suitable normalization, a possible set of standard modes is given by

$$\Phi_m(z) = \frac{1}{m^2}\sin\left(\frac{m\pi(z + H_0)}{H_0}\right)$$

in which case the coefficients σ_{jk} become

$$\sigma_{jk} = \frac{2}{jk}c_1^2.$$

This result can also be obtained from the WKB case with $\xi = 2N_b/\overline{N} = 2$ since $N_b = N$ when N^2 is constant. The resulting coefficients for the matrix M_n are $m_{jk} = c_1^2(2 + \delta_{j,k}))/jk$, where $\delta_{j,k}$ is the Kronecker δ. If we denote by R_1 the eigenvector of M_n associated with the largest eigenvalue, the expression for $\Phi_{1,\rm new}'(z)$ is thus

$$\Phi_{1,\rm new}'(z) = \frac{\pi}{H_0}\sum_{j=1}^{n}\frac{R_{j,1}}{j}\cos\left(\frac{j\pi(z + H_0)}{H_0}\right). \tag{61}$$

The coefficients $R_{j,1}$were estimated numerically, as well as the sum (61). We find empirically that n = 300 is more than sufficient for reaching numerical convergence. In this case, we find that the resulting vertical structure is indistinguishable from that given by the following analytical expression (up to an unimportant multiplicative constant):

$$\Phi_{1,\rm new}'(z) = -\frac{\pi}{2H_0}\sin\left(\frac{\pi(z + H_0)}{2H_0}\right) + \frac{1}{H_0}, \tag{62}$$

hence $\Phi_{1,\rm new}(z) = \cos[\pi(z + H_0)/2H_0] + z/H_0$. Interestingly, the function $\Phi_{1,\rm new}(z) - z/H_0 = \cos[\pi(z + H_0)/$

$2H_0$] can be obtained from the standard Sturm-Liouville problem by changing the bottom boundary condition to $\Phi'(-H_0) = 0$ instead of $\Phi(-H_0) = 0$, that is, by replacing the condition of vanishing vertical velocity by that of vanishing bottom pressure.

c. Eigenmode with zero bottom pressure

The previous result suggests that there is a link between $\Phi_{1,\mathrm{new}}(z)$ and the gravest eigenmode $\mathcal{V}$ of the Sturm-Liouville problem

$$\frac{d^2\mathcal{V}}{dz^2} + \frac{N^2}{\gamma^2}\mathcal{V} = 0, \tag{63}$$

with boundary conditions $\mathcal{V}(0) = 0$, $d\mathcal{V}/dz(-H_0) = 0$, such that

$$\mathcal{V} = \underbrace{\sum_{m=1}^{+\infty} \alpha_m \Phi_m(z)}_{\Phi_{1,\mathrm{new}}(z)} + Az. \tag{64}$$

By construction, this expression satisfies the upper and lower boundary conditions provided that the constant A is taken as

$$A = -\sum_{m=1}^{+\infty} \alpha_m \Phi_m'(-H_0). \tag{65}$$

As a result, (64) becomes

$$\mathcal{V} = \sum_{m=1}^{+\infty} \alpha_m(\Phi_m(z) - \Phi_m'(-H_0)z). \tag{66}$$

In order to determine the coefficients α_m, (66) is inserted into the Sturm-Liouville problem (63). This yields the following problem:

$$\sum_{m=1}^{+\infty} \alpha_m\left(\frac{1}{\gamma^2} - \frac{1}{c_m^2}\right)N^2\Phi_m = \frac{1}{\gamma^2}\sum_{m=1}^{+\infty} \alpha_m\Phi_m'(-H_0)N^2z. \tag{67}$$

After projection onto the basis of the Φ_m one obtains

$$\begin{aligned}\alpha_n\left(\frac{1}{\gamma^2} - \frac{1}{c_n^2}\right)\int_{-H_0}^0 N^2(z)\Phi_n^2(z)\,dz \\ = \frac{1}{\gamma^2}\sum_{m=1}^{+\infty} \alpha_m\Phi_m'(-H_0)\int_{-H_0}^0 zN^2\Phi_n(z)\,dz.\end{aligned} \tag{68}$$

The latter integral can be simplified by using the relationship $N^2\Phi_n = -c_n^2\Phi_m''$ and integrating by parts so that

$$\begin{aligned}\int_{-H_0}^0 zN^2(z)\Phi_n(z)\,dz &= -c_n^2\int_{-H_0}^0 z\Phi_n''(z)\,dz \\ &= -c_n^2\Phi_n'(-H_0)H_0.\end{aligned} \tag{69}$$

After some manipulation, the above system can be rewritten as follows:

$$\sum_{m=1}^{+\infty} \sigma_{mn}\alpha_m + c_n^2\alpha_n = \gamma^2\alpha_n \tag{70}$$

with

$$\sigma_{mn} = \frac{\Phi_m'(-H_0)\Phi_n'(-H_0)}{\int_{-H_0}^0 N^2\Phi_n^2\,dz}H_0c_n^4. \tag{71}$$

By using (39) [with $\Phi_j(0) = 0$, $j \geq 1$, using the rigid-lid approximation], one realizes that (71) is identical to the expression for σ_{jk} (42) originally derived in section 3. This establishes that the anomalous phase speeds can, in fact, also be determined by solving the modified Sturm-Liouville problem (63). The main interest of this result is to offer a computationally efficient way to compute the anomalous phase speeds that is much cheaper than using the series expansion introduced in section 3. On the other hand, the latter series expansion remains the better way to get approximate theoretical results for the anomalous phase speeds. The reason is that WKB theory does not seem to work satisfactorily on the modified Sturm-Liouville problem for reasons that appear related to the bottom pressure boundary condition. Similar difficulties were encountered by Killworth and Blundell (1999) (Killworth 1999, personal communication) to compute approximate solutions for the WKB modes over topography.

5. Interpretation of TOPEX/Poseidon measurements

We test the relevance of the pressure-decorrelation theory by comparing its predicted amplification factors with the ratios of observed to standard phase speed from Chelton and Schlax (1996), as well as with the ratio predicted by the mean-flow theory reported in Killworth et al. (1997). The extended Levitus dataset (Boyer and Levitus 1997) is used for the computation in the regions investigated by Chelton and Schlax (1996). The amplification factors predicted by WKB theory are compared with those predicted by solving the Sturm-Liouville problem with a vanishing bottom pressure instead of a vanishing vertical velocity.

a. Predictions of WKB theory

Values of the ratio $N_b/\overline{N}$ are easily estimated from hydrographic data, allowing us to compute the amplification factor for the global ocean by using the computational relationship obtained for $n = 300$ (the upper curve depicted in Fig. 2). The dataset used is the Levitus climatology extended to ¼° resolution by Boyer and Levitus (1997). The result, shown in Fig. 4, demonstrates that the amplification factor thus obtained in the midlatitudes has a value around 2. Values close to 3 are obtained in the regions of the Antarctic Circumpolar Current, as well as in the subpolar gyre in the North

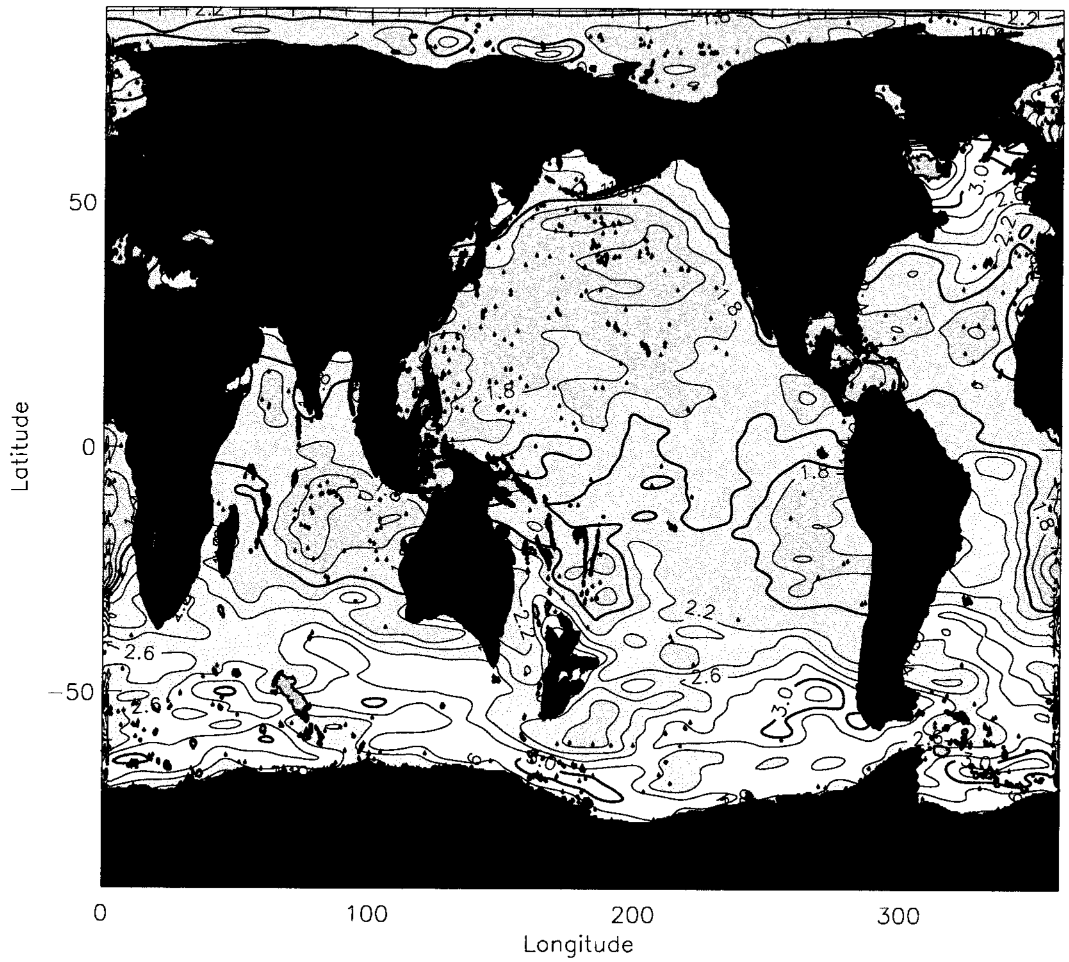

FIG. 4. Global map of the theoretical enhancement factor, $1 + 2N_b\overline{N}$, computed from the extended Levitus 94 climatology. Modest smoothing has been applied. Regions in black (other than continents) correspond to data with singular behavior (e.g., negative buoyancy frequency at some level or excessive shallowness for our analysis to be meaningful). The contour interval is 0.2, and the thick contour represents an amplification factor of 2.0.

Atlantic, due to the weak stratification that exists there; this implies high values for the ratio $N_b/\overline{N}$. The ratio $N_b/\overline{N}$ is strongly affected by topographic features so that the original map at the ¼° resolution of the extended Levitus dataset is quite noisy. The small scales are filtered by successive application of a 5° averaging filter in longitude, and a 1° averaging filter in latitude.

Estimates of the zonal phase speed from TOPEX/Poseidon altimetric data are generally determined from use of the radon transform at a given latitude over longitudinal bands spanning approximately 30°. Amplification factors are computed over the same longitudinal bands and displayed in Fig. 1 (top). For comparison, the results of the standard theory are displayed in Fig. 1 (bottom), and the results of the mean-flow theory are displayed in Fig. 1 (middle). A logarithmic scale is used so that overestimates are put on the same footing as underestimates. The standard theory clearly underestimates the observations. The mean-flow theory does better, but still underestimates observations. In contrast, the present theory overestimates observations, with discrepancy similar in magnitude to that of the mean-flow theory. Error bars are computed as one standard deviation of our estimates for the amplification factor over the aforementioned longitudinal bands.

b. Predictions of exact asymptotic theory

The above comparison is repeated with the amplification factors computed from solving the Sturm-Liouville problem with a vanishing bottom pressure instead of a vanishing vertical velocity. This method was shown in the previous section to yield the asymptotic value of the anomalous phase speed due to bottom pressure decorrelation; therefore, its predictions are intrinsically more accurate than those of WKB theory. The modified Sturm-Liouville problem was solved by interpolating N on a regular vertical grid every $\Delta z = 20$ m. Given the greatly increased computational cost of this approach compared to that of the WKB method, we solved the

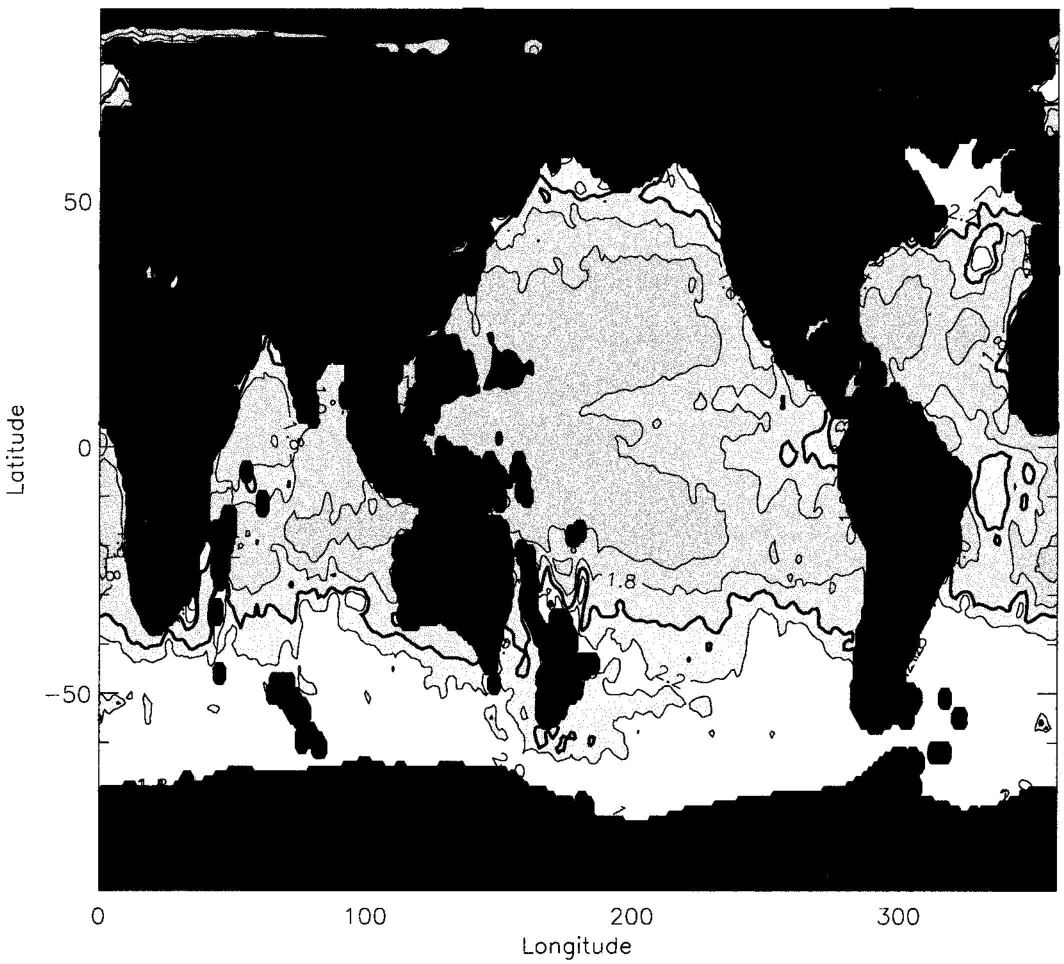

FIG. 5. Same as in Fig. 4 but with the theoretical enhancement factor computed by solving the Sturm-Liouville problem with a bottom boundary condition of vanishing bottom pressure instead of vanishing vertical velocity. [The Levitus (1994) analysis grid is subsampled by a factor of four in each direction by averaging N profiles over 1° square boxes.] The contour intervals is the same as in the previous figure but the levels of gray are different. White areas denote regions with amplification factor greater than 2.2.

above eigenvalue problem on a $1° \times 1°$ grid, obtained by averaging our $¼° \times ¼°$ N vertical profiles dataset on one-degree square boxes. The result, shown in Fig. 5, shows significantly smoother patterns than Fig. 4, with values generally smaller than those predicted by WKB theory. For instance, amplification factors in the North Pacific are about 0.2 less than with the WKB method. However, both approaches appear consistent with each other, in the sense that they both show systematically higher amplification factors in the southern Hemisphere than in the Northern Hemisphere, in agreement with the Chelton and Schlax (1996) findings.

Although the two approaches yield somewhat different looking patterns on the global maps of Figs. 4 and 5, we find little differences between the two methods when restricting the comparison to the regions analyzed by Chelton and Schlax (1996), as depicted in Fig. 6 (note that the lower panel of Fig. 6 is the same as the upper panel of Fig. 1). Indeed, the main difference appears in the error bars, which are smaller for the asymptotic theory owing to lesser variance and resolution.

As an additional comparison between the two methods, we depicted in Fig. 7 a nonsmoothed longitudinal section of the deep Brunt–Väisälä frequency around 35°N (top panel), along with the theoretical phase-speed enhancement predicted by the asymptotic ''exact'' and zero-order WKB theories (bottom panel). The latter shows that WKB estimates are closely related to that of the deep Brunt–Väisälä frequency, as theory suggests, whereas such sensitivity is absent in the other theory. The two methods have both significant differences, but without any obvious bias between them, and many regions where they roughly coincide. Therefore, it appears difficult to say when WKB theory will overestimate the asymptotic ''exact'' theory and conversely. Nevertheless, even though WKB theory may not always be accurate, it does capture the phase-speed enhancement resulting from bottom pressure decorrelation at very little

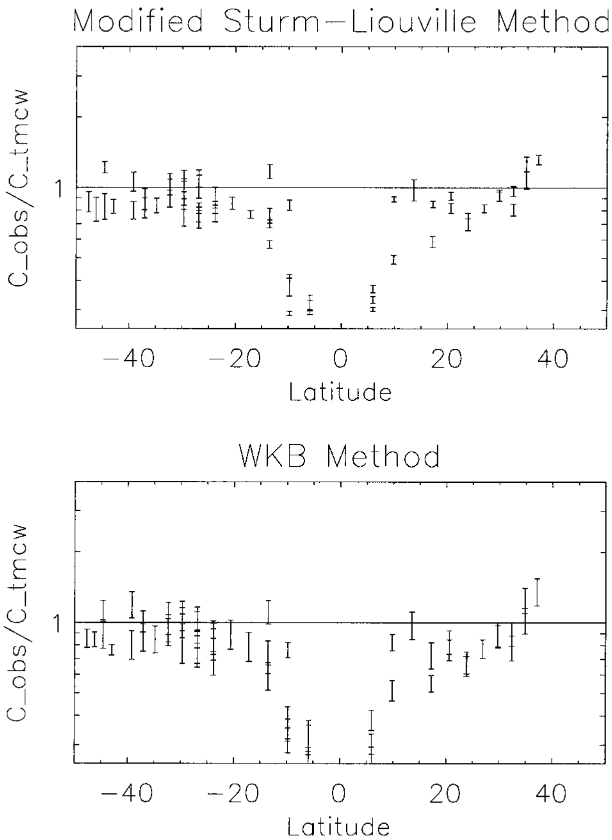

FIG. 6. The ratio of observed to theoretical phase speed for the present theory computed from solving the (top) modified Sturm-Liouville problem and (bottom) by using WKB theory. Note that the bottom panel is the same as the upper panel of Fig. 1.

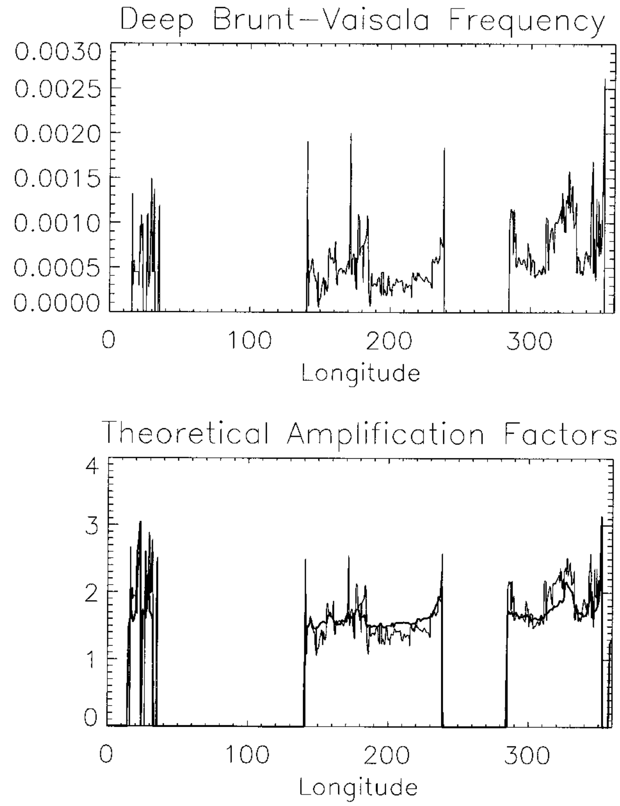

FIG. 7. (top) Zonal section of the deep Brunt–Väisälä frequency (in s^{-1}) at 35°N. The nonvanishing values correspond to the Mediterranean, Pacific, and Atlantic, respectively, from left to right. (bottom) Zonal section of the theoretical amplification factor at the same latitude: zero-order WKB theory, $1 + 2N_b/\overline{N}$ (thin solid line), and prediction obtained from solving the modified Sturm-Liouville problem (thick solid line).

computational cost, with the additional advantage of relating the amplification factor to observable physical quantities in a simple way.

6. Discussion

The main result of this paper is to quantify the phase-speed enhancement that occurs when the bottom pressure fluctuations are decoupled from the overlaying ocean dynamics in a continuously stratified fluid. When WKB theory is applicable in the vertical direction, the amplification factor has a particularly simple form that depends only on the ratio of the deep Brunt–Väisälä frequency to its vertical average. Results are also established for more general conditions, but they are more difficult to interpret physically. In particular, we formally show that the amplification factor can be very generally related at leading order to the bottom value of the vertical modal function for the first baroclinic standard mode. We also show that the faster phase speeds can be obtained by solving the Sturm-Liouville problem for the standard modes by replacing the bottom condition of zero vertical velocity with that of vanishing pressure. Thus, the faster modes are related to the classical theoretical surface-intensified modes believed to occur over steep topography.

Although regarding the faster modes and phase speeds as solutions of the modified Sturm-Liouville problem may appear much simpler than regarding them as asymptotic solutions of a series expansion in terms of the standard modes, we believe this is only advantageous from a numerical viewpoint. Indeed, it turns out that the eigenmodes of the modified Sturm-Liouville problem are very difficult to study analytically, except in the very idealized case of a constant Brunt–Väisälä frequency. In particular, we failed to find approximate WKB solutions for realistic N^2 profiles. Apparently, Killworth and Blundell (1999) encountered the same problem (Killworth 1999, personal communication) when attempting to find approximate WKB solutions to the vertical modes over slowly varying topography.

The physical mechanism responsible for the phase-speed enhancement is the dynamical coupling between the standard modes that can occur in a realistic ocean because of the violation of the basic assumptions made in the standard theory. In this paper we make the ad hoc assumptions that this coupling is independent of time and location and that the normal modes cancel each other exactly at the ocean bottom. In this respect, this paper extends to a continuously stratified fluid the well-known result that baroclinic Rossby waves are faster in a reduced-gravity, layered model than in the same model with all the layers active.

Of course, the assumption of a time- and spatially independent coupling between the standard modes is an idealization unlikely to occur in the real ocean. Still, we find evidence in the literature—albeit indirect and based on fragmentary results of numerical calculations, theory, and laboratory experiments—that it is not an unreasonable one. Our theoretical predictions outside the tropical band (10°S–10°N) show reasonable agreement with observational estimates. In contrast to the mean-flow theory whose estimates are generally systematically too low, ours are generally too high. On the other hand, since the assumption of total bottom pressure decorrelation is probably an exaggeration, then a more realistic, partial decorrelation will cause a somewhat smaller phase speed enhancement that is even closer to the observational estimates. Even so, the discrepancy with the observational estimates, assuming total decorrelation, is no greater than the discrepancy for the mean-flow theory.

As it now stands our theory remains speculative in part because the nature of the decorrelation is assumed rather than deduced directly from the equations of motion. In order to achieve further progress one needs to understand how other effects like nonlinearities, forcing, and friction affect the coupling among vertical modes. Further research on this topic might give a better understanding of the pressure decorrelation mechanisms, as well as of the limits of validity in assuming a deep resting layer in layered models of the ocean.

Acknowledgments. We thank Dudley Chelton for kindly providing his data and for frequent discussions about phase-speed enhancement. We thank Peter Killworth for interesting exchanges and two anonymous reviewers for thorough comments and suggestions that helped improve the manuscript. This research was supported by the National Science Foundation through Grant OCE-9633681 and the National Aeronautics and Space Administration through Grant NAG5-3982.

APPENDIX

WKB Approximation of σ_{jk}

As Eq. (44) shows, the determination of the coefficients σ_{jk} requires an explicit knowledge of the standard baroclinic modes. Here, we use WKB theory to compute approximate expressions for the solution $\Phi_m(z)$ of the Sturm-Liouville problem (10)–(11) by following the methodology recently used by Chelton et al. (1998). To be valid, WKB requires a scale separation between N/c_m and Φ_m. Mathematically, this is generally verified if for all m,

$$\frac{1}{N^2}\left(\frac{dN}{dz}\right)^2 \ll \frac{N^2}{c_m^2}, \qquad \frac{1}{N}\frac{d^2N}{dz^2} \ll \frac{N^2}{c_m^2}. \tag{A1}$$

Since c_m decreases as the number of nodes of Φ_m increases, the approximation is expected to improve as m increases. In Chelton et al. (1998) the authors found that WKB theory gave satisfactory results for the first baroclinic mode, even though realistic N^2 profiles rarely strictly comply with (A1), with a maximum error around 10%. The so-called physical optics approximation for Φ_m is given by

$$\Phi_m(z) = B_m\left[\frac{N(z)}{c_m}\right]^{-1/2} \sin\left(\frac{1}{c_m}\int_{-H_0}^{z} N(\zeta)\, d\zeta\right), \tag{A2}$$

where B_m is an arbitrary constant. The corresponding approximation for $\Phi'_m(z)$ is obtained by taking the vertical derivative of (A2),

$$\Phi'_m(z) = -\frac{B_m}{2}\left[\frac{N(z)^3}{c_m}\right]^{-1/2} N'(z)\sin\left(\frac{1}{c_m}\int_{-H_0}^{z} N(\zeta)\, d\zeta\right) + B_m\left[\frac{N(z)}{c_m}\right]^{1/2} \cos\left(\frac{1}{c_m}\int_{-H_0}^{z} N(\zeta)\, d\zeta\right). \tag{A3}$$

An additional classical approximation consists in making the rigid-lid approximation $\Phi_m(0) = 0$ for the baroclinic modes ($m \geq 1$) (Gill 1982). From (A2), this imposes

$$c_m = \frac{1}{m\pi}\int_{-H_0}^{0} N(z)\, dz = \frac{\overline{N}H_0}{m\pi}, \tag{A4}$$

denoting by $\overline{N}$ the vertical average of N.

In order to estimate σ_{jk} from (44), we use (A2) to first compute

$$\int_{-H_0}^{0} N^2\Phi_m^2\, dz = c_m B_m^2 \int_{-H_0}^{0} N(z)\sin^2\left(\frac{1}{c_m}\int_{-H_0}^{z} N(\zeta)\, d\zeta\right) dz. \tag{A5}$$

Using the identity $\sin^2 x = (1 - \cos 2x)/2$, it comes

$$\int_{-H_0}^{0} N^2\Phi_m\, dz = \frac{B_m^2 c_m^2 m\pi}{2} - \frac{B_m^2 c_m^2}{4}\int_{-H_0}^{0} \frac{2N(z)}{c_m}\cos\left(\frac{2}{c_m}\int_{-H_0}^{z} N(\zeta)\, d\zeta\right) dz. \tag{A6}$$

The last integral vanishes because its integrand is of the form $\cos u u' = (\sin u)'$ so that

$$\int_{-H_0}^{0} N^2 \Phi_m^2 \, dz = \frac{B_m^2 c_m^2 m\pi}{2} = \frac{B_m^2 H_0^2 \overline{N}^2}{2m\pi}, \qquad \text{(A7)}$$

using (A4). Now, by using the equivalence relation (39) between the norms of Φ and Φ', accounting for the rigid-lid approximation, one obtains

$$\int_{-H_0}^{0} \Phi_m'^2 \, dz = \frac{B_m^2 m\pi}{2}. \qquad \text{(A8)}$$

From (A3), one computes $\Phi_m'(-H_0) = B_m(N_b/c_m)^{1/2}$, where $N_b = N(-H_0)$ denotes the bottom value of the buoyancy frequency. By inserting this result in combination with (A8) into (44), the resulting WKB approximation for σ_{jk} is given by

$$\sigma_{jk} = 2\frac{H_0}{\pi}\frac{\sqrt{c_j c_k} N_b}{\sqrt{jk}} = \frac{2N_b}{\overline{N}}\frac{1}{jk}c_1^2, \qquad \text{(A9)}$$

since from (A4), one has $c_1 = H_0\overline{N}/\pi$ and thus $c_m = c_1/m$.

REFERENCES

Boyer, T. P., and S. Levitus, 1997: *Objective Analyses of Temperature and Salinity for the World Ocean on a 1/4 Degree Grid.* NOAA Atlas NESDIS, 11.

Charney, J. G., and G. Flierl, 1981: Oceanic analogues of atmospheric motions. *Evolution of Physical Oceanography,* B. A. Warren and C. Wunsch, Eds., The MIT Press, 504–548.

Chelton, D. B., and M. G. Schlax, 1996: Global observations of oceanic Rossby waves. *Science,* **272,** 234–238.

——, R. A. de Szoeke, M. G. Schlax, K. E. Naggar, and N. Siwertz, 1998: Geographical variability of the first baroclinic Rossby radius of deformation. *J. Phys. Oceanogr.,* **28,** 433–460.

de Szoeke, R. A., and D. Chelton, 1999: The enhancement of planetary wave speeds by homogeneous potential vorticity layers. *J. Phys. Oceanogr.,* **29,** 500–511.

Dewar, W. K., 1998: On ''too fast'' baroclinic planetary waves in the general circulation. *J. Phys. Oceanogr.,* **28,** 1739–1758.

Flierl, G. R., 1978: Models of vertical structure and the calibration of two-layer models. *Dyn. Atmos. Oceans,* **2,** 341–381.

Garrett, C., P. MacCready, and P. Rhines, 1993: Boundary mixing and arrested Ekman layers—Rotating stratified flow near a sloping boundary. *Annu. Rev. Fluid Mech.,* **25,** 291–323.

Gill, A., 1982: *Dynamics of Atmospheres and Oceans.* Academic Press, 662 pp.

Hallberg, R., 1997: Localized coupling between the surface and bottom-intensified flow over topography. *J. Phys. Oceanogr.,* **27,** 977–998.

Hong, B. G., W. Sturges, and A. J. Clarke, 1998: Decadal wind forcing of the North Atlantic subtropical gyre. *J. Phys. Oceanogr.,* **28,** 659–668.

Killworth, P. D., and J. R. Blundell, 1999: The effect of bottom topography on the speed of long extratropical planetary waves. *J. Phys. Oceanogr.,* **29,** 2689–2710.

——, D. Chelton, and R. A. de Szoeke, 1997: The speed of observed and theoretical long extratropical planetary waves. *J. Phys. Oceanogr.,* **27,** 1946–1966.

Liu, Z. Y., 1999: Planetary waves in the thermocline: Non-doppler-shift mode, advective mode and green mode. *Quart. J. Roy. Meteor. Soc.,* **125,** 1315–1339.

McWilliams, J. C., P. R. Gent, and N. Norton, 1986: The evolution of balanced, low-mode vortices on the β-plane. *J. Phys. Oceanogr.,* **16,** 838–855.

Mellor, G. L., and X. H. Wang, 1996: Pressure compensation and the bottom boundary layer. *J. Phys. Oceanogr.,* **26,** 2214–2222.

Qiu, B., W. Miao, and P. Müller, 1997: Propagation and decay of forced and free baroclinic rossby waves in off-equatorial oceans. *J. Phys. Oceanogr.,* **27,** 2405–2417.

Reznik, G. M., and T. V. Tsybaneva, 1994: On the influence of topography and stratification on planetary waves in the ocean (two-layer model). *Oceanology,* **34,** 1–9.

Rhines, P. B., 1970: Edge-, bottom-, and Rossby waves in a rotating stratified fluid. *Geophys. Fluid Dyn.,* **1,** 273–302.

——, 1975: Waves and turbulence on a beta-plane. *J. Fluid Mech.,* **69,** 417–443.

——, 1977: The dynamics of unsteady currents. *The Sea.* Vol. 6: *Marine Modeling.* E. Goldberg et al., Eds., Wiley, 189–318.

Samelson, R. M., 1992: Surface-intensified Rossby waves over rough topography. *J. Mar. Res.,* **50,** 367–384.

Straub, D. N., 1994: Dispersion of Rossby waves in the presence of zonally varying topography. *Geophys. Astrophys. Fluid Dyn.,* **75,** 107–130.

Tailleux, R., and J. C. McWilliams, 2000: Acceleration, creation, and depletion of wind-driven, baroclinic Rossby waves over an ocean ridge. *J. Phys. Oceanogr.,* **30,** 2186–2213.

Veronis, G., 1981: Dynamics of large-scale circulation. *Evolution of Physical Oceanography,* B. A. Warren and C. Wunsch, Eds., The MIT Press, 140–183.

White, W. B., 1977: Annual forcing of baroclinic long waves in the tropical North Pacific Ocean. *J. Phys. Oceanogr.,* **7,** 50–61.

——, Y. Chao, and C. Tai, 1997: Coupling of biennal oceanic Rossby waves with the overlying atmosphere in the Pacific basin. *J. Phys. Oceanogr.,* **27,** 1236–1251.

Zang, X. Y., and C. Wunsch, 1999: The observed dispersion relationship for North Pacific Rossby wave motions. *J. Phys. Oceanogr.,* **29,** 2183–2190.